Commun Nonlinear Sci Numer Simulat 84 (2020) 105175

Contents lists available at ScienceDirect

Commun Nonlinear Sci Numer Simulat

journal homepage: www.elsevier.com/locate/cnsns

Research paper

Time delayed chemical synapses and synchronization in multilayer neuronal networks with ephaptic inter-layer coupling

Mohadeseh Shafiei[a], Sajad Jafari[a], Fatemeh Parastesh[a], Mahmut Ozer[b,c], Tomasz Kapitaniak[d], Matjaž Perc[e,f,g,*]

[a] Department of Biomedical Engineering, Amirkabir University of Technology, 424 Hafez Ave., Tehran 15875-4413, Iran
[b] Ministry of National Education, Ankara 06420, Turkey
[c] Center for Artificial Intelligence and Data Science, Istanbul Technical University, Istanbul 34469, Turkey
[d] Division of Dynamics, Technical University of Lodz, Stefanowskiego 1/15, Lodz 90-924, Poland
[e] Faculty of Natural Sciences and Mathematics, University of Maribor, Koroška cesta 160, Maribor 2000, Slovenia
[f] Department of Medical Research, China Medical University Hospital, China Medical University, Taichung, Taiwan
[g] Complexity Science Hub Vienna, Josefstädterstraße 39, Vienna 1080, Austria

ARTICLE INFO

Article history:
Received 14 August 2019
Revised 30 December 2019
Accepted 6 January 2020
Available online 08 January 2020

Keywords:
Multilayer network
Ephaptic coupling
Time delay
Synchronization

ABSTRACT

In this paper, a three-layer neuronal network is studied to consider different complex connections between the neurons. In the nervous system, the communication between the neurons is mostly based on the electrical and chemical synapses. However, extracellular electric fields can induce a magnetic flux which can lead to indirect neural communications, by means of electromagnetic induction. This mode of coupling is called ephaptic coupling, which here is used between the layer. To describe the coupling within the layers, the electrical and chemical synapses are defined. We also take into account the partial time delays, to reflect the required time for information transmission through chemical synapses. Particularly, we consider partial and full time delays, as well as strong and weak coupling strengths. It is shown that three layers typically have opposite synchronization properties in the strong and weak coupling regimes. Specifically, when the coupling is strong, the top and bottom layers are synchronous, while the middle layer is desynchronous. But when the coupling is weak, the middle layer is synchronous, while the top and bottom layers are desynchronous. In overall, the most synchrony is obtained when the weak coupling is accompanied with partial time delays in chemical communications. Our research sheds new light on the complex interplay between the time delay, the ephaptic coupling, and the synchronization in neuronal networks.

1. Introduction

Complex networks have been widely studied for their widespread uses in different sciences such as biology and engineering [1]. The study of characteristics of complex networks helps in better understanding of real systems and phenomena [2,3]. Synchronization is one of the essential collective behaviors, which has been extensively studied in complex networks, such

* Corresponding author.
E-mail addresses: matjaz.perc@um.si, matjaz.perc@uni-mb.si (M. Perc).

https://doi.org/10.1016/j.cnsns.2020.105175
1007-5704/

as neuronal networks [4–6]. Synchronization phenomena can play a crucial role in the functionality of the brain [7]. Majority of the studies on neuronal networks have considered full synchronization, in which all the neurons exhibit completely the same behavior [8–10]. However, other synchronization patterns, such as phase synchronization, cluster synchronization, lag synchronization, solitary states, and chimera states, have also been studied [11–14]. These patterns have closer relations with the synchronization patterns in the brain [12,15,16]. In a network of identical oscillators, chimera state represents a spatiotemporal pattern with the coexistence of synchronized and desynchronized regions [3,17–20]. Chimera state has been found in natural phenomena, such as uni-hemispheric sleep in birds and dolphins, and also in some brain disorders such as schizophrenia or epileptic seizures [21–24].

In most of the previous studies, the communications between the neurons have been considered to be via chemical or electrical synapses [22,25]. Electrical connections occur through gap junctions, and inhibitory/excitatory connections occur via chemical synapses [26]. The chemical synapse refers to the transmission of neurotransmitters from the pre-synaptic cell to the post-synaptic one, which takes a delay of several milliseconds [26]. The presence of synapses plays a decisive role in transferring the signals between the neurons. However, there is another kind of non-synaptic communication, known as the ephaptic coupling that describes the extracellular signal communication [27–29]. In this type of communication, the ionic flows in the neuron activity induce some alternations in the extracellular voltage of the cell membrane. Therefore, it can lead to an electrical field and also change the excitability of neighboring neurons [14,30–32]. Each of the signal transmission paths has a unique task in the nervous system and the overall communications are conducted through the mixture of these transmissions. Therefore, studying the complex behavior of the neuronal networks with simultaneous consideration of synaptic and non-synaptic communications, seems very consequential.

Recently, multilayer networks have attracted considerable attention for their potential ability in modeling the real-world complex systems with different levels of connectivity [33–35]. Given the structural and functional characteristics of the neuronal network, the provision of the multilayer based models can be reasonable. It can also help in understanding the intricate connections in neuronal data transmissions [35]. Majhi et al. studied a two-layer network of Hindmarsh–Rose neurons, with one layer composed of uncoupled neurons (without direct connections) and one layer formed of coupled neurons via electrical connections [36]. By considering the chemical synapses between the two layers, they showed that the indirect connections between the uncoupled neurons can lead to chimera state in the uncoupled layer. Xu et al. considered a multilayer memristive neuronal network of modified Hindmarsh–Rose neurons. Their system was consisted of two layers, where the neurons in each layer were coupled with bidirectional electrical synapses, and two layers were coupled with memristive synapses[37]. They reported that the memristive synapses have a notable influence on the synchronization of the network, and by adjusting the coupling strength, chimera state can be achieved. They also showed that the presence of delay in the inter-layers couplings, has a significant role in the emergence of chimera state.

The studies have revealed the effects of transmission time delay on the synchronization patterns of the neuronal networks [10,38,39]. The time delay has a substantial impact on the dynamics of neurons' firing, spiking rate, the degree of phase synchronization, and transition between different synchronization states [16,40–43]. It has been suggested that the fixed, distributed, or time-varying time delay can be a factor for controlling the chimera states' characteristics [44,45]. Wang et al. [46] investigated scale-free neuronal networks of coupled Rulkov maps and reported that the information transmission time delay plays a crucial role in the transition of different synchronization patterns, in both attractively and repulsively coupled networks. Also, they showed that in the small-world network of Morris-Lecar neurons, the network could restore synchronized activity, when the time delay in connections was short or moderate. However, longer delay leaded to anti-phase synchronization and clustering [47].

In this paper, a three-layer neuronal network is considered, where the bottom and top layers have electrical synaptic communications, and the intermediate layer has chemical synapses. The inter-layer connections are deemed to occur through the ephaptic couplings. It is also supposed that the chemical communications in the intermediate layer occur with some time delay. There are two control parameters, the time delay (τ), and the probability of the presence of time delay in the connections (P_d), to study the role of partial time delay in the emergence of different patterns. Particularly, We consider two cases of full time delay, when all connections are subjected to delay, and partial time delay, when only some connections are subjected to delay. We investigate how delay in the chemical synaptic connections can alter the synchronization, not only in the middle layer but also in the two other layers indirectly. In the second section, the dynamic of the proposed network is presented in detail. Section three presents a method for measuring the phase synchronization. The numerical simulation representation and the discussion of the results are given in section four. Eventually, the conclusions are given in section five.

2. System dynamics

A multilayer network composed of three layers is investigated. In the top and bottom layers, the neurons are connected via electrical synapses, and in the intermediate layer, the connections are through chemical synapses. Since in chemical synapses' signaling, the neurotransmitters are transferred from presynaptic to postsynaptic neurons, chemical connections have some time delay, which is considered in the model. Due to considering the effects of the magnetic field, a modified Hindmarsh–Rose model is used. In 2016, Lv and Ma [50] presented this new model by adding a new variable to the well-known Hindmarsh–Rose model which describes the magnetic flux. This model is capable of exhibiting vibrant and complex

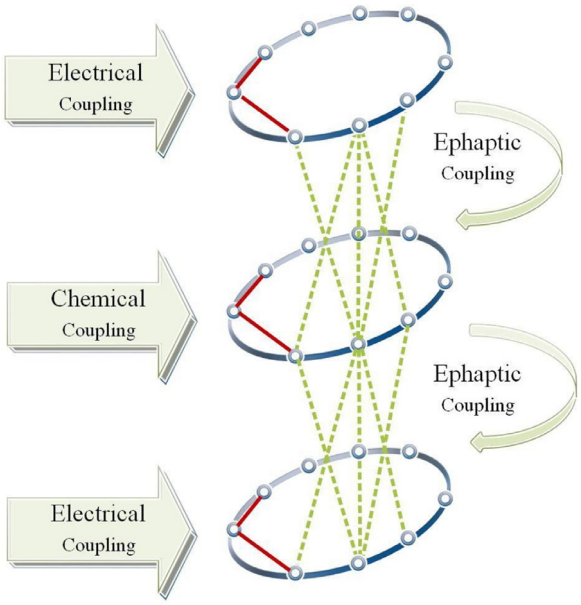

Fig. 1. The schematic diagram of a multilayer network with three layers. The neurons in the top and bottom layers are coupled with electrical synapses and in the intermediate layer, are coupled through chemical synapses. Each neuron in the middle layer is connected via bidirectional magnetic connections to its corresponding neighboring neurons in two other layers.

dynamical behaviors of the neuron. The modified HR model is as follows:

$$\begin{aligned}
\dot{x} &= f(x,y,z,\varphi) = y - ax^3 + bx^2 - z + I_{ext} - k_1 w(\varphi)x \\
\dot{y} &= g(x,y,z,\varphi) = c - dx^2 - y \\
\dot{z} &= h(x,y,z,\varphi) = r(s(x - x_0) - z) \\
\dot{\varphi} &= u(x,y,z,\varphi) = x - k_2\varphi \\
w(\varphi) &= \alpha + 2\beta\varphi^2
\end{aligned} \tag{1}$$

Fig. 1 shows the schematic of the three-layer network. The top and bottom layers are assumed to be connected with the intermediate layer, by bidirectional inter-layer magnetic couplings. The mathematical equations of the top and bottom layers are presented by:

$$\begin{aligned}
\dot{x_{i1}} &= f(x_{i1}, y_{i1}, z_{i1}, \varphi_{i1}) + g_e \sum_{j=1}^{N} A_{i,j}(x_{j1} - x_{i1}) \\
\dot{y_{i1}} &= g(x_{i1}, y_{i1}, z_{i1}, \varphi_{i1}) \\
\dot{z_{i1}} &= h(x_{i1}, y_{i1}, z_{i1}, \varphi_{i1}) \\
\dot{\varphi_{i1}} &= u(x_{i1}, y_{i1}, z_{i1}, \varphi_{i1}) + g_m \sum_{j=1}^{N} A_{i,j}(\varphi_{j2} - \varphi_{i1})
\end{aligned} \tag{2}$$

$$\begin{aligned}
\dot{x_{i3}} &= f(x_{i3}, y_{i3}, z_{i3}, \varphi_{i3}) + g_e \sum_{j=1}^{N} A_{i,j}(x_{j3} - x_{i3}) \\
\dot{y_{i3}} &= g(x_{i3}, y_{i3}, z_{i3}, \varphi_{i3}) \\
\dot{z_{i3}} &= h(x_{i3}, y_{i3}, z_{i3}, \varphi_{i3}) \\
\dot{\varphi_{i3}} &= u(x_{i3}, y_{i3}, z_{i3}, \varphi_{i3}) + g_m \sum_{j=1}^{N} A_{i,j}(\varphi_{j2} - \varphi_{i3})
\end{aligned} \tag{3}$$

and for the intermediate layer, the model is described as,

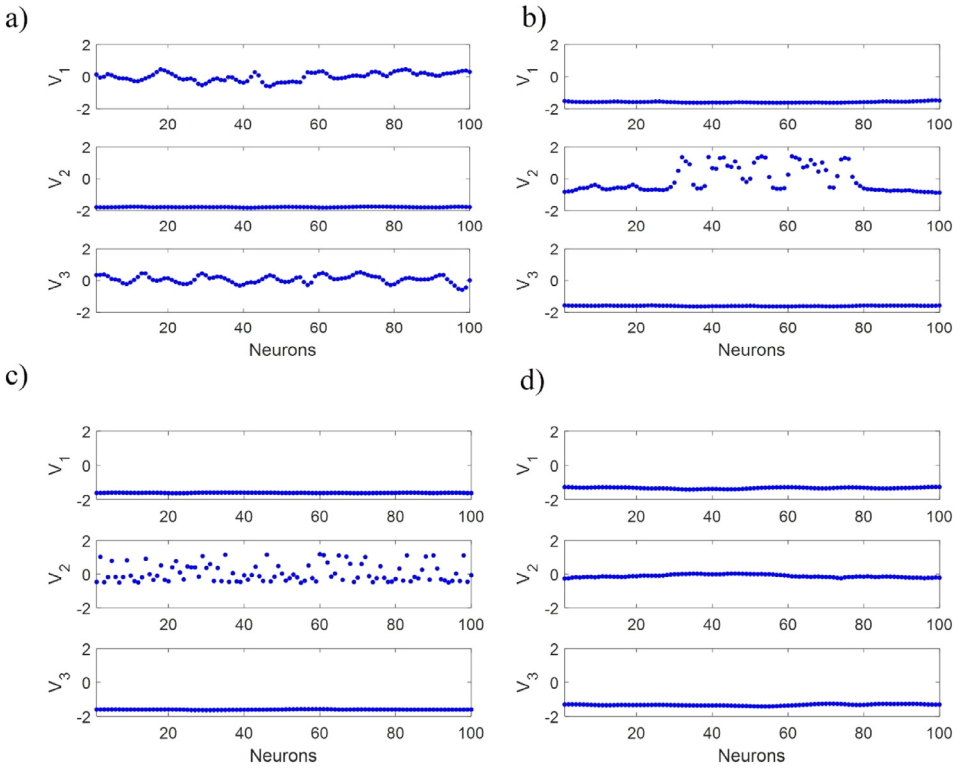

Fig. 2. The snapshots of the membrane potentials of three layers' neurons, at $t = 3000$, with $P_d = 1$, $g_m = 1$, $g_e = 0.5$, $g_{ch} = 0.05$. (a) $\tau = 0.1$: layer I, III are phased synchronized and layer II is zero-lag synchronized, (b) $\tau = 1.4$: layer I, III are zero-lag synchronized and layer II shows chimera state, (c) $\tau = 2$: layer I, III are zero-lag synchronized and layer II is incoherent, (d) $\tau = 5$: all layers are zero-lag synchronized. The figure shows that in a strongly coupled network, in the case of full-time delay, the upper and lower layers are more synchronous than the middle layer, and the change in the latency of the network makes it possible to take different synchronization patterns in the middle layer.

$$
\begin{aligned}
\dot{x_{i2}} &= f(x_{i2}, y_{i2}, z_{i2}, \varphi_{i2}) + g_{ch} \sum_{j=1}^{N} A_{i,j}(v_s - x_{i2})\Gamma(x_{i2}(t-\tau)) \\
\dot{y_{i2}} &= g(x_{i2}, y_{i2}, z_{i2}, \varphi_{i2}) \\
\dot{z_{i2}} &= h(x_{i2}, y_{i2}, z_{i2}, \varphi_{i2}) \\
\dot{\varphi_{i2}} &= u(x_{i2}, y_{i2}, z_{i2}, \varphi_{i2}) + g_m \sum_{j=1}^{N} A_{i,j}(\varphi_{j1} + \varphi_{j3} - 2\varphi_{i2}) \\
\Gamma(x) &= \frac{1}{1 + e^{-\lambda(x-\theta_s)}}
\end{aligned}
\tag{4}
$$

where the variables x, y, z, and φ represent the membrane potential, slow current for recovery variables, adaption current and magnetic flux across the membrane, respectively. I_{ext} describes the external forcing current. $w(\varphi) = \alpha + 3\beta\varphi^2$ is the memory conductance of flux-controlled memristor, that represents the coupling between x and φ variables, where α and β are constant parameters [28,48].

The subscript i, and j represent the ith, and jth neuron, respectively, where $i, j = 1, 2, ..., N$ with N being the total number of neurons in each layer. $A = [A_{i,j}]$ is the zero-row sum coupling matrix, such that $A_{i,j} = 1$ if the i^{th} neuron is connected to the j^{th} neuron and otherwise $A_{i,j} = 0$. Neurons in each layer, are considered to be on a ring, where each neuron interacts with its nearest neighbors on each side. Also, each neuron in the middle layer interacts ephaptically with its three corresponding nearest neighboring neurons in two other layers (see Fig. 1). g_m, g_e, and g_{ch} are the magnetic, electrical and chemical coupling strengths, respectively. $\Gamma(x)$ is the activation function, in which λ is a positive constant and θ_s is the threshold [36]. If $v_s > x_i$, the synapses are excitatory and here we choose $v_s = 2$ (excitatory connections) for all connections [12]. τ is the time delay that takes nonzero values with the probability P_d. The parameters are chosen at $a = 1$, $b = 3$, $c = 1$, $d = 5$, $r = 0.006$, $s = 4$, $k_1 = 1$, $k_2 = 0.5$, $I_{ext} = 2.2$, $\lambda = 100$, $\theta_s = -0.25$, $\alpha = 0.1$ and $\beta = 0.02$. By considering this set of parameters (inspired from previous studies [12,16,48]) the behavior of the isolated neuron is regular spiking. The initial conditions for delayed equations are selected randomly from uniform distribution in the interval [0,1].

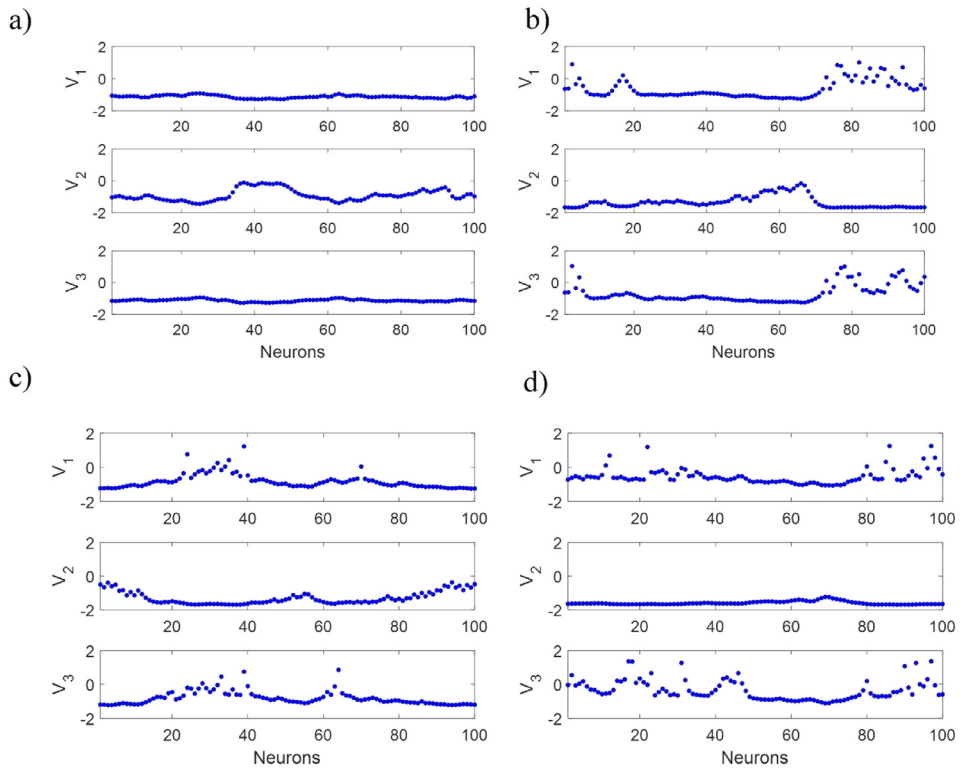

Fig. 3. The snapshots of the membrane potentials of three layers' neurons, at $t = 3000$, with $P_d = 1$, $g_m = 0.1$, $g_e = 0.05$, $g_{ch} = 0.005$. (a) $\tau = 0.1$: layer I, III are zero-lag synchronized and layer II is phase synchronized, (b) $\tau = 1.4$: layer I, III show chimera state and layer II is phase synchronized, (c) $\tau = 2$: layer I, III show imperfect chimera state and layer II is phase synchronized, (d) $\tau = 5$: layer I, III show chimera state and layer II is zero-lag synchronized. The figure indicates that in a weak-coupling network, in the case of full-time delay, the middle layer is more synchronous than the upper and lower layers. Increasing the latency makes the first and third layers more incoherent.

3. Phase synchronization measure

The timing of the single spikes has some information about neuronal communications. Parameter R is used to quantify the degree of phase synchronization and describes the collective behavior of spike trains [49]. The parameter R is defined as,

$$R = \frac{1}{N}\left|\sum_{j=1}^{N} exp(i\theta_j(t))\right| \tag{5}$$

where $\theta_j(t)$ is the phase for the jth neuron at the time t and is determined as:

$$\theta_j(t) = 2\pi \frac{t - t_{j,k}}{t_{j,k+1} - t_{j,k}}$$
$$j = 1, ..., N \tag{6}$$

where $t_{j,k}$ is the starting time of the kth spike of the jth neuron. To find the starting times numerically, a threshold has been defined and the peaks of the neurons' firing time series have been detected. Zero R indicates no synchronization, and $R = 1$ shows complete synchronization [10].

4. Results

In the following, the results of considering time delay in the chemical synapses of the intermediate layer's connections are presented. The study is performed on the network with both strong and weak couplings. Numerical results are generated by using the 4th order Runge–Kutta estimation method with $timestep = 0.1$. In reporting the results, we have selected the set of parameters which has more effects on the behavior of the neurons, and also satisfies the reproducibility of the patterns.

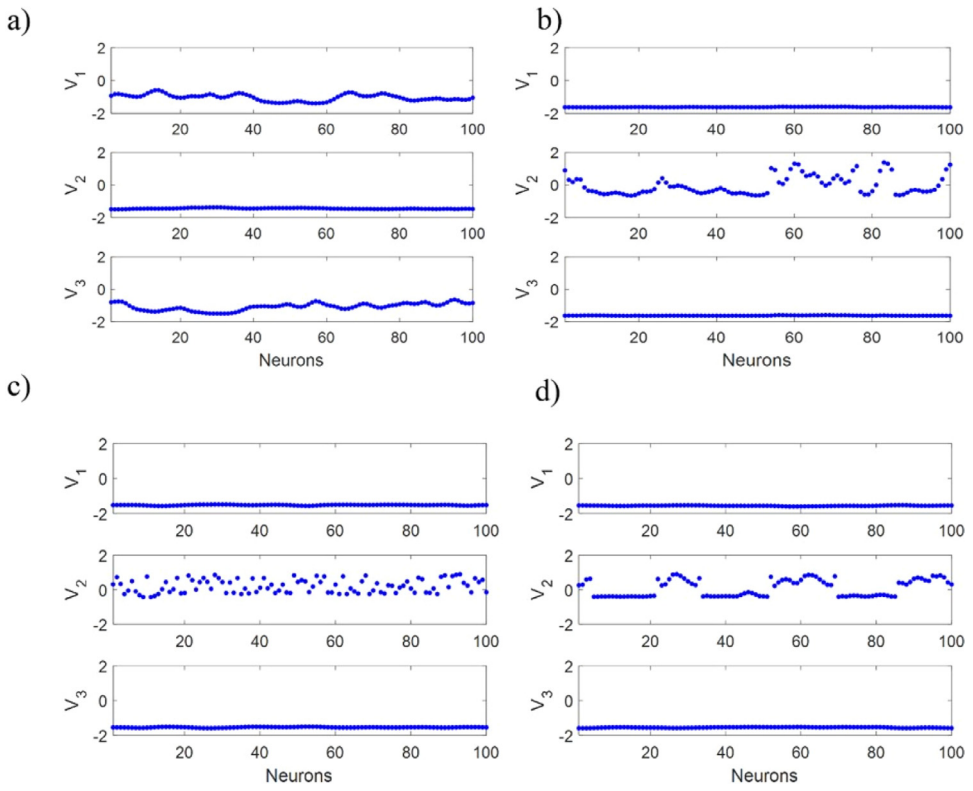

Fig. 4. The snapshots of the membrane potentials of three layers' neurons, at $t = 3000$, with $P_d = 0.5$, $g_m = 1$, $g_e = 0.5$, $g_{ch} = 0.05$. (a) $\tau = 1.6$: layer I, III are phase synchronized and layer II is zero-lag synchronized, (b) $\tau = 2$: layer I, III are zero-lag synchronized and layer II shows chimera state, (c) $\tau = 2.2$: layer I, III are zero-lag synchronized and layer II is incoherent, (d) $\tau = 3.2$: layer I, III are zero-lag synchronized and layer II shows solitary states. The figure suggests that in a strong-coupling network, in the case of full-time delay, the middle layer is more asynchronous than the upper and lower layers. The partial time delay can change the level of synchronization of the network pattern in the second layer.

4.1. Full-time delay

The snapshots of the membrane potentials of three layers' neurons of the network at $t = 3000$ are presented in Figs. 2, and 3, for different values of τ at $P_d = 1$, in strong and weak coupling strengths, respectively. Fig. 2 shows the network patterns when the coupling strengths are set at $g_m = 1$, $g_e = 0.5$, $g_{ch} = 0.05$, which refers to as strong couplings. This figure shows that varying the time delay makes transitions between different spatiotemporal patterns alternately. In detail, the snapshots of the three layers are ordered when $\tau = 0.1$. In this case, the neurons in the top and bottom layers have similar ordered patterns of firing, since they have the same type of intra-layer electrical couplings (see Fig. 2 panel (a)). As the connections are delayed with relatively small τ, the layer I and III are phase synchronized, and layer II is zero-lag synchronized. The phase synchronized state is a continuous snapshot pattern which indicates that the neurons of the network fire by specific phase difference with their neighboring neurons, and in the zero-lag synchronized, all neurons have the same membrane voltage level at a particular moment in the snapshot, which means that all the neurons in the middle layer fire and come to rest, simultaneously.

When τ increases to $\tau = 1.4$, the ordered patterns of layer I and III are maintained ordered, but layer II pattern becomes rather disordered (see Fig. 2 panel (b)). The snapshots in Fig. 2b suggest that layer I and III tend to zero-lag synchronization, while layer II shows the coexistence of coherent and incoherent regions, that is known as chimera state. As τ increases to $\tau = 2$, layer I and III maintain their order, while layer II becomes notably disordered (see Fig. 2 panel (c)). The snapshots shown in Fig. 2c, determine that layer I and II are zero-lag synchronized and layer II is desynchronized. As τ increases to larger values of $\tau = 5$, it can be seen that the multilayer network is again moving toward coherent states (see Fig. 2 panel (d)). The snapshots in Fig. 2d indicate that all layers are zero-lag synchronized. Fig. 2 illustrates that full time delayed intralayer connections in layer II, can have a remarkable influence on the synchronization patterns of the multilayer network. It seems that increasing or decreasing the delay can be a factor to control the degree of the multilayer network's synchronization.

Let consider another full-time delay case, where the network has weak coupling strengths as $g_m = 0.1$, $g_e = 0.05$, $g_{ch} = 0.005$. The most noticeable point about this network is that the middle layer is generally more synchronous than the upper and lower layers. Some results of this case are represented in Fig. 3. When $\tau = 0.1$, the network shows the ordered patterns

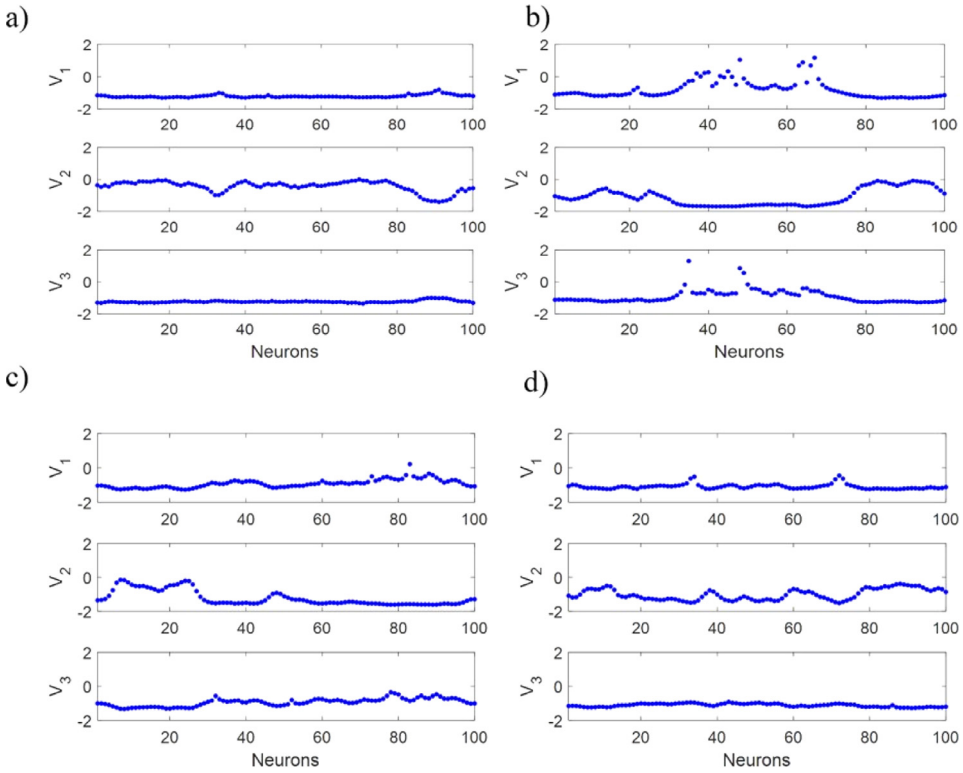

Fig. 5. The snapshots of the membrane potentials of three layers' neurons, at t = 3000, with $P_d = 0.5$, $g_m = 0.1$, $g_e = 0.05$, $g_{ch} = 0.005$. (a) $\tau = 2$: layer I, III are zero-lag synchronized and layer II is phase synchronized, (b)$\tau = 3$: layer I, III show chimera state and layer II is phase synchronized, (c) $\tau = 3.9$: all layers are phase synchronized, (d) $\tau = 5$: all layers are phase synchronized. The figure confirms that in a weak-coupling network, in the case of partial time delay, the middle layer is more synchronous than the upper and lower layers. In this case, the network is more synchronized than in the previous cases.

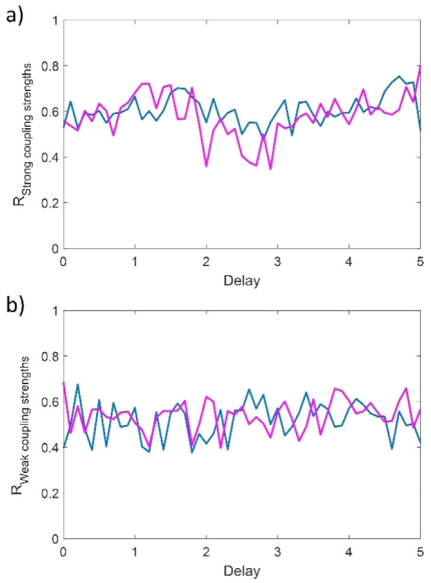

Fig. 6. Dependence of parameter R on the time delay τ, for the full and partial time delay (magenta and blue color respectively). (a) Strong coupling strengths: $g_m = 1$, $g_e = 0.5$, $g_{ch} = 0.05$. (b) Weak coupling strengths: $g_m = 0.1$, $g_e = 0.05$, $g_{ch} = 0.005$. This figure represents the nonlinear changes in R by increasing the delay. The minimum values of this curve are the values of delays in which layer II has less synchrony.

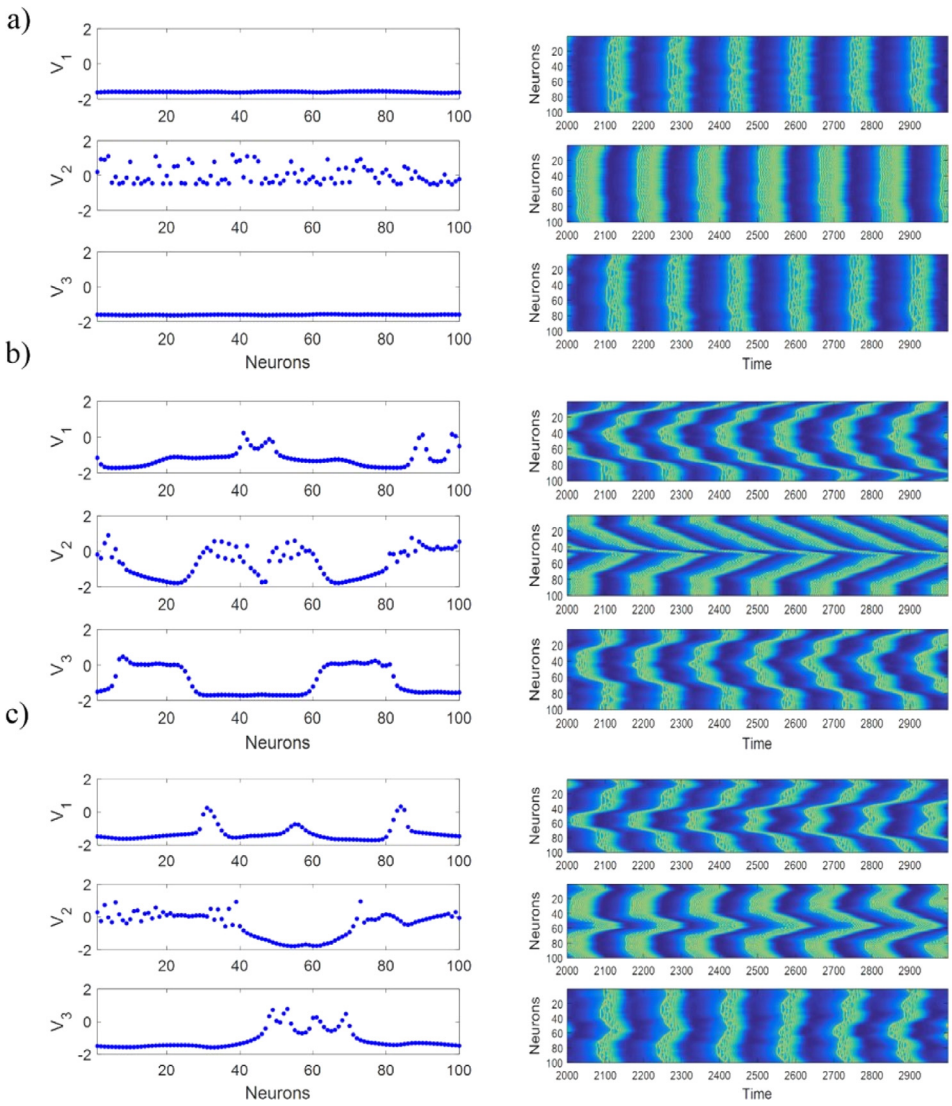

Fig. 7. The spatiotemporal patterns and snapshots of the membrane potentials of three layers' neurons, at $t = 3000$, with $P_d = 1$, $g_m = 1$, $g_e = 0.5$, $g_{ch} = 0.05$. (a) $\tau = 2.2$: layer I, III are zero-lag synchronized and layer II is incoherent, (b) $\tau = 2.7$: layer I, III show phase synchronized patterns and layer II is chimera states, (c) $\tau = 2.9$: layer I, III show phase synchronized patterns and layer II is chimera states. This figure shows the relevance between minimums of parameter R and network synchronization in layer II for the full-time delays and strong coupling strengths.

in all three layers (see Fig. 3 panel (a)). The snapshots in Fig. 3a confirms that layer I and III are zero-lag phase synchronized and layer II is phase synchronized. This state indicates an interesting result: in this case, compared to the previous one with strong couplings, the type of synchronization pattern of the middle layer is displaced with two other layers. When τ is increased to $\tau = 1.4$, the ordered snapshot patterns of layer I and III, become disordered, while layer II sustains its order (see Fig. 3 panel (b)). In this case, the snapshot patterns in layer I and III indicate chimera state, while layer II is phase synchronized again. Further increase of time delay does not change the pattern of layer II but makes the patterns of the other layers change to imperfect chimera state (see Fig. 3 panel (c)). In this special case, some neurons suddenly break the continuous coherent group and have different firings. Fig. 3d shows the network pattern for $\tau = 5$. It represents that, in contrast to the multilayer network with strong coupling strengths, when the delay increases, the layers I and III are not synchronized anymore, and they maintain in chimera state. On the other hand, layer II tends to have a zero-lag synchronized pattern. It can be concluded that the multilayer network with full-time delay, is more desynchronized in weak coupling strengths in comparison to strong ones.

4.2. Partial time delay

Some previous studies reveal that in real neuronal networks, only some of the connections are subjected to delay [16,51]. Therefore, we consider a probability (P_d) for the delayed connections and set it at $P_d = 0.5$ as an average value. The results

of this case when the couplings are strong, are presented in Fig. 4. It can be found that similar to the previous strong case (see Fig. 2), the upper and lower layers are generally more synchronous than the middle layer. When $\tau = 1.6$, the layer I and III are phase synchronized and layer II is zero-lag synchronized (see Fig. 4 panel (a)). When τ increases to $\tau = 2$, layer I and III keep their ordered patterns, while the ordered pattern of layer II becomes semi-disordered (see Fig. 4 panel (b)). In this case, the chimera state is seen in layer II. As τ increases to $\tau = 2.2$, (see Fig. 4 panel (c)) synchronization regions of the layer II become desynchronized and chimera state disappears. Therefore, the snapshots in Fig. 4c depicts incoherent regions. If we increase the delay to $\tau = 3.3$, as before, layer I and III will be synchronous. In this case, synchronization pattern of layer II is the solitary state, possessing a few isolated neurons in the network with the remaining neurons experiencing cluster synchronization [21](see Fig. 4 panel (d)).

Fig. 5 indicates the results of the network for partial time delay with weak coupling strengths. As can be predicted from the previous results, the middle layer is more synchronous than two other layers, in weak coupling strengths. Fig. 5a refers to the time delay $\tau = 2$, in which the network layers maintain their order for larger amounts of the time delay, in comparison to the previous case (see Fig. 4). Fig. 5a shows that layer I and III are zero-lag synchronized, and layer II is phase synchronized. As τ increases to $\tau = 3$, (see Fig. 5 panel (b)) synchronization regions of the layers I and III become desynchronized, and chimera state appears. In this case, layer II is phase synchronized. If we increase the delay to $\tau = 3.9$, all layers are phase synchronized (see Fig. 5 panel (c)). For a larger amount of time delay, all layers are phase synchronized again (see Fig. 5 panel (d)). The observations indicate that the network with weak coupling strengths and partial time delays in chemical synapses is further synchronized.

4.3. Parameter R quantification

In order to quantify the influence of the full and partial time delays for the network with both strong and weak coupling strengths, we calculate the dependence of parameter R on the time delay at $P_d = 1$ and $P_d = 0.5$. The results are presented in Fig. 6. This figure shows that R changes nonlinearly by increasing the delay. The minimum values of this curve represent the values of delays in which the middle layer has less synchrony. For example, the parameter R has three minimum points for a network with strong coupling strengths in full-time delay mode. To examine the status of the middle layer of the network, for these three delay values, the time snapshots and spatiotemporal patterns of the network are illustrated in Fig. 7.

Fig. 7 shows that the intermediate layer has a desynchronized pattern for all of the specified delay values. Fig. 7 panel (a) refers to the first minimum point of the parameter R, which is at $\tau = 2$. In this case, layer I and III are zero-lag synchronized, and layer II is incoherent. The second minimum point is $\tau = 2.7$. For this delay value, as shown in Fig. 7b, layer I and III are phase synchronized, while layer II represents a chimera state. The largest delay for the most desynchronization in the second layer of the network is at $\tau = 2.9$. In this case, the snapshots and spatiotemporal patterns of network suggest that layer I and III are phase synchronized, and layer II is in the chimera state (see Fig. 7 panel (c)).

5. Conclusion

In this paper, a multilayer neuronal network composed of three layers was investigated. The modified Hindmarsh-Rose neuron, which can describe the magnetic flux, was used as the single units of the network. We considered three layers to describe different communications in neural transmissions. The neurons in the top and bottom layers were coupled via electrical synapses and in the middle layer were coupled through chemical synapses. The top and bottom layers were connected with the middle layer via indirect ephaptic coupling, which refers to electromagnetic induction. All of the connections of the neurons were considered to be local. The partial time delay was also supposed in the middle layer to define the time delay occurring in the chemical synapse signal transmission. The time delay was encountered in two cases of full-time delay, where all the connections have time delay, and partial time delay with the probability of $P_d = 0.5$. The network patterns were investigated by varying the coupling strengths. Almost in all the simulations, the top and bottom layers had the same behaviors that is due to their similar structures and connections. The results showed different patterns in strong and weak couplings. Indeed, when the couplings are strong, the top and bottom layers were synchronous, whereas the middle one was not and exhibited different patterns of asynchronization or chimera state, by varying the time delay. When the couplings were weakened, the middle layer became synchronized. In this case, changing the time delay induced asynchronization or chimera state in the top and bottom layers. In overall, employing weak couplings with partial time delay, was the most synchronizable case.

Declaration of Competing Interest

The authors declare that they have no known competing financial interests or personal relationships that could have appeared to influence the work reported in this paper.

CRediT authorship contribution statement

Mohadeseh Shafiei: Project administration, Formal analysis, Software, Validation, Writing - original draft. **Sajad Jafari:** Project administration, Formal analysis, Software, Validation, Writing - original draft. **Fatemeh Parastesh:** Project administration, Formal analysis, Software, Validation, Writing - original draft. **Mahmut Ozer:** Project administration, Formal analysis, Software, Validation, Writing - original draft. **Tomasz Kapitaniak:** Project administration, Formal analysis, Software, Validation, Writing - original draft. **Matjaž Perc:** Project administration, Formal analysis, Software, Validation, Writing - original draft.

Acknowledgements

Matjaž Perc was supported by the Slovenian Research Agency (Grants J4-9302, J1-9112 and P1-0403).

References

[1] Boccaletti S, Latora V, Moreno Y, Chavez M, Hwang DU. Complex networks: Structure and dynamics. Phys Rep 2006;424(4-5):175–308.
[2] Ma J, Tang J. A review for dynamics in neuron and neuronal network. Nonlinear Dyn 2017;89(3):1569–78.
[3] Ma J, Tang J. A review for dynamics of collective behaviors of network of neurons. Sci China Technol Sc 2015;58(12):2038–45.
[4] Jalili M. Neuronal synchronization over networks with small-world property. In: Information Management and Engineering, 2009. ICIME'09. International Conference on IEEE. IEEE; 2009. p. 17–21.
[5] Krishnagopal S, Lehnert J, Poel W, Zakharova A, Schöll E. Synchronization patterns: from network motifs to hierarchical networks. Phil Trans R Soc A 2017;375(2088):20160216.
[6] Wang C, Ma J. A review and guidance for pattern selection in spatiotemporal system. Int J Mod Phys A 2018;32(06):1830003.
[7] Mathalon DH, Sohal VS. Neural oscillations and synchrony in brain dysfunction and neuropsychiatric disorders: it's about time. JAMA Psychiat 2015;72(8):840–4.
[8] Rakshit S, Bera BK, Ghosh D. Synchronization in a temporal multiplex neuronal hypernetwork. Phys Rev E 2018;98(3):032305.
[9] Tang J, Ma J, Yi M, Xia H, Yang X. Delay and diversity-induced synchronization transitions in a small-world neuronal network. Phys Rev E 2011;83(4):046207.
[10] Wang Q, Perc M, Duan Z, Chen G. Synchronization transitions on scale-free neuronal networks due to finite information transmission delays. Phys Rev E 2009;80(2):026206.
[11] Bera BK, Ghosh D, Lakshmanan M. Chimera states in bursting neurons. Phys Rev E 2016;93(1):012205.
[12] Jalili M. Spike phase synchronization in multiplex cortical neural networks. Physica A 2017;466:325–33.
[13] Maistrenko Y, Penkovsky B, Rosenblum M. Solitary state at the edge of synchrony in ensembles with attractive and repulsive interactions. Phys Rev E 2014;89(6):060901.
[14] Majhi S, Ghosh D. Alternating chimeras in networks of ephaptically coupled bursting neurons. Chaos 2018;28(8):083113.
[15] Penn Y, Segal M, Moses E. Network synchronization in hippocampal neurons. Proc Natl Acad Sci 2016;113(12):3341–6.
[16] Sun X, Perc M, Kurths J. Effects of partial time delays on phase synchronization in watts-strogatz small-world neuronal networks. Chaos 2017;27(5):053113.
[17] Bera BK, Majhi S, Ghosh D, Perc M. Chimera states: Effects of different coupling topologies. Europhys Lett 2017;118(1):10001.
[18] Dudkowski D, Maistrenko Y, Kapitaniak T. Occurrence and stability of chimera states in coupled externally excited oscillators. Chaos 2016;26(11):116306.
[19] Gambuzza LV, Buscarino A, Chessari S, Fortuna L, Meucci R, Frasca M. Experimental investigation of chimera states with quiescent and synchronous domains in coupled electronic oscillators. Phys Rev E 2014;90(3):032905.
[20] Parastesh F, Jafari S, Azarnoush H, Hatef B, Bountis A. Imperfect chimeras in a ring of four-dimensional simplified lorenz systems. Chaos Solitons Fractals 2018;110:203–8.
[21] Majhi S, Kapitaniak T, Ghosh D. Solitary states in multiplex networks owing to competing interactions. Chaos 2019;29(1):013108.
[22] Chouzouris T, Omelchenko I, Zakharova A, Hlinka J, Jiruska P, Schöll E. Chimera states in brain networks: Empirical neural vs. modular fractal connectivity. Chaos 2018;28(4):045112.
[23] Majhi S, Perc M, Ghosh D. Chimera states in a multilayer network of coupled and uncoupled neurons. Chaos 2017;27(7):073109.
[24] Wei Z, Parastesh F, Azarnoush H, Jafari S, Ghosh D, Perc M, Slavinec M. Nonstationary chimeras in a neuronal network. Europhys Lett (EPL) 2018;123(4):48003.
[25] Ma J, Tang J. A review for dynamics in neuron and neuronal network. Nonlinear Dyn 2017;89(3):1569–78.
[26] Pereda A, Faber DS. Two forms of electrical transmission between neurons. Front Mol Neurosci 2018;11:427.
[27] Han K-S, Guo C, Chen CH, Witter L, Osorno T, Regehr WG. Ephaptic coupling promotes synchronous firing of cerebellar purkinje cells. Neuron 2018;100(3):564–78.
[28] Ma J, Mi L, Zhou P, Xu Y, Hayat T. Phase synchronization between two neurons induced by coupling of electromagnetic field. Appl Math Comput 2017;307:321–8.
[29] Martinez-Banaclocha M. Ephaptic coupling of cortical neurons: possible contribution of astroglial magnetic fields? Neuroscience 2018;370:37–45.
[30] Zhang Y, Tsang TK, Bushong EA, Chu L-A, Chiang A-S, Ellisman MH, Reingruber J, Su CY. Asymmetric ephaptic inhibition between compartmentalized olfactory receptor neurons. Nat Commun 2019;10(1):1560.
[31] Mondal A, Upadhyay RK, Ma J, Yadav BK, Sharma SK, Mondal A. Bifurcation analysis and diverse firing activities of a modified excitable neuron model. Cogn Neurodyn 2019:1–15.
[32] Xu Y, Jia Y, Ma J, Hayat T, Alsaedi A. Collective responses in electrical activities of neurons under field coupling. Sci Rep 2018;8(1):1349.
[33] Boccaletti S, Bianconi G, Criado R, Genio CID, Gómez-Gardenes J, Romance M, Sendina-Nadal I, Wang Z, Zanin M. The structure and dynamics of multilayer networks. Phys Rep 2014;544(1):1–122.
[34] Kivelä M, Arenas A, Barthelemy M, Gleeson JP, Moreno Y, Porter MA. Multilayer networks. J Complex Networks 2014;2(3):203–71.
[35] Vaiana M, Muldoon SF. Multilayer brain networks. J Nonlinear Sci 2018:1–23.
[36] Majhi S, Perc M, Ghosh D. Chimera states in uncoupled neurons induced by a multilayer structure. Sci Rep 2016;6:39033.
[37] Xu F, Zhang J, Jin M, Huang S, Fang T. Chimera states and synchronization behavior in multilayer memristive neural networks. Nonlinear Dyn 2018;94(2):775–83.
[38] Burić N, Todorović K, Vasović N. Synchronization of bursting neurons with delayed chemical synapses. Phys Rev E 2008;78(3):036211.
[39] Shafiei M, Parastesh F, Jalili M, Jafari S, Perc M, Slavinec M. Effects of partial time delays on synchronization patterns in izhikevich neuronal networks. Eur Phys J B 2019;92(2):36.
[40] Bolhasani E, Azizi Y, Valizadeh A, Perc M. Synchronization of oscillators through time-shifted common inputs. Phys Rev E 2017;95(3):032207.

[41] Çakir Y. Modeling of time delay-induced multiple synchronization behavior of interneuronal networks with the izhikevich neuron model. Turk J Electr Eng Co 2017;25(4):2595–605.
[42] Gu H, Zhao Z. Dynamics of time delay-induced multiple synchronous behaviors in inhibitory coupled neurons. PLoS One 2015;10(9):e0138593.
[43] Rossoni E, Chen Y, Ding M, Feng J. Stability of synchronous oscillations in a system of hodgkin-huxley neurons with delayed diffusive and pulsed coupling. Phys Rev E 2005;71(6):061904.
[44] Gjurchinovski A, Schöll E, Zakharova A. Control of amplitude chimeras by time delay in oscillator networks. Phys Rev E 2017;95(4):042218.
[45] Zakharova A, Semenova N, Anishchenko V, Schöll E. Time-delayed feedback control of coherence resonance chimeras. Chaos 2017;27(11):114320.
[46] Wang Q, Chen G, Perc M. Synchronous bursts on scale-free neuronal networks with attractive and repulsive coupling. PLoS one 2011;6(1):e15851.
[47] Wang Q, Perc M, Duan Z, Chen G. Impact of delays and rewiring on the dynamics of small-world neuronal networks with two types of coupling. Physica A 2010;389(16):3299–306.
[48] Panahi S, Jafari S, Khalaf AJM, Rajagopal K, Pham V-T, Alsaadi FE. Complete dynamical analysis of a neuron under magnetic flow effect. Chin J Phys 2018;56(5):2254–64.
[49] Jalili M. Phase synchronizing in hindmarsh–rose neural networks with delayed chemical coupling. Neurocomputing 2011;74(10):1551–6.
[50] Lv M, Ma J. Multiple modes of electrical activities in a new neuron model under electromagnetic radiation. Neurocomputing 2016;250:375–81.
[51] Yan H, Sun X. Impact of partial time delay on temporal dynamics of watts–strogatz small-world neuronal networks. Int J Bifurcation Chaos 2017;27(07):1750112.